

Irreversible Pressure-Induced Transformation of Boron Nitride Nanotubes

Surajit Saha¹, Vikram Gadagkar¹, Prabal K. Maiti², D. V. S. Muthu¹, D. Golberg³,
C. Tang³, C. Zhi³, Y. Bando³, and A. K. Sood^{1,*}

¹Department of Physics, Indian Institute of Science, Bangalore 560012, India

²Centre for Condensed Matter Theory, Department of Physics, Indian Institute of Science, Bangalore 560012, India

³National Institute for Materials Science, Tsukuba, Ibaraki 305-0044, Japan

We have used Raman spectroscopy to study the behavior of multi-walled boron nitride nanotubes and hexagonal boron nitride crystals under high pressure. While boron nitride nanotubes show an irreversible transformation at about 12 GPa, hexagonal boron nitride exhibits a reversible phase transition at 13 GPa. We also present molecular dynamics simulations which suggest that the irreversibility of the pressure-induced transformation in boron nitride nanotubes is due to the polar nature of the bonds between boron and nitrogen.

Keywords: Boron Nitride Nanotube, High Pressure Raman, Molecular Dynamics.

1. INTRODUCTION

Mechanical properties of carbon nanotubes have been of tremendous interest in recent years for the development of ultra-strong nanotube composites. Several experimental^{1,2} and theoretical^{3–5} studies have contributed to the understanding of these properties. Hexagonal boron nitride (h-BN), which is an analogue of semi-metallic graphite, is a material with several potential applications. The interest in h-BN has been fortified with the synthesis of boron nitride nanotubes. Boron nitride nanotubes were discovered by Chopra et al.⁶ just after the theoretical prediction by Rubio et al.⁷ Being wide band gap (~5.7 eV) semiconductors, boron nitride nanotubes are potential materials for nanoelectronics as well as for optoelectronics, UV light sources, and detectors. To understand the mechanical properties of these materials, we have done high pressure Raman experiments on multi-walled boron nitride nanotubes and molecular dynamics simulations on single-walled boron nitride nanotubes and compared them with those on carbon nanotubes. The crucial difference between boron nitride and carbon nanotubes is the polar vis-a-vis non-polar nature of bonds in these materials.

2. EXPERIMENTAL DETAILS

Multi-walled nanotubes of boron nitride were prepared by chemical vapor deposition using carbon free precursors

*Author to whom correspondence should be addressed.

and catalysts as described by Tang et al.⁸ Characterization of the nanotubes were done by Electron Energy Loss Spectroscopy (EELS) and High-Resolution Transmission Electron Microscopy (HRTEM) which indicate that multi-walled nanotubes are composed of boron and nitrogen with a B to N ratio of ~1 ($\pm 20\%$) and are typically 5–15 coaxial tubes with outer diameters ranging from 20–50 nm.

High pressure Raman experiments at room temperature were carried out on multi-walled boron nitride nanotubes up to 16 GPa and on h-BN up to 21 GPa. A tiny speck of the sample was loaded in a hole of ~200 μm diameter drilled in a pre-indented stainless steel gasket of a Mao-Bell type diamond anvil cell with methanol, ethanol, and water mixture in the ratio 16:3:1 as the pressure transmitting medium. Raman spectra were recorded in backscattering geometry using the 514.5 nm line of an argon ion laser.

3. SIMULATION METHODOLOGY

We have used DREIDING,⁹ a standard generic macromolecular force field, in all our molecular dynamics (MD) simulations. Table I lists the force field parameters used to calculate intra- and inter-molecular interactions. We have previously used this force field to study the collapse of single and double-walled carbon nanotube bundles under hydrostatic pressure.⁵ Our simulations were performed using MODULASIM,¹⁰ a modular and general purpose molecular modeling package. The ensemble used was one of constant particle number, pressure, and temperature (NPT). The temperature (300 K) and the applied

Table I. Parameters for the B (B_2) and N (N_R) atom types, in DREIDING [10], a standard generic macromolecular force field used in all our molecular dynamics simulations. X denotes an arbitrary atom.

$E_{\text{bond}}(R) = 1/2 K_b (R - R_0)^2$	N-B	R_0	1.43 Å	K_b	1400 kcal/mol/Å ²
$E_{\text{angle}}(\theta) = 1/2 K_\theta (\cos \theta - \cos \theta_0)^2$	X-B-X	θ_0	120°	K_θ	100 kcal/mol/rad ²
	X-N-X	θ_0	120°	K_θ	100 kcal/mol/rad ²
$E_{\text{torsion}}(\phi) = 1/2 V \{1 - \cos[n(\phi - \phi_0)]\}^2$	X-N-B-X	Φ_0	180°	V	25 kcal/mol, $n = 2$
$E_{\text{inverse}}(\psi) = K_i (\cos \psi - \cos \psi_0)^2 / (\sin \psi_0)^2 / 2$	B-X-X-X	$\Psi_0 (B_2)$	0°	K_i	40 kcal/mol/rad ²
	N-X-X-X	$\Psi_0 (N_R)$	0°	K_i	40 kcal/mol/rad ²
$E_{\text{vdW}} = D_0 \{(R_0/R)^{12} - (R_0/R)^6\}$	B	$R_0 (B_2)$	4.0200 Å	D_0	0.0950 kcal/mol
	N	$R_0 (N_R)$	3.6621 Å	D_0	0.0774 kcal/mol
$E_Q = 322.0637 (Q_i Q_j / \epsilon R_{ij})$	B	Q	+0.6767e ⁺		
	N	Q	-0.6767e ⁺		

hydrostatic pressure were maintained using the Berendsen thermostat and barostat.¹¹ The electrostatic part of the potential was calculated using two different approaches—a crude cutoff method (cutoff radius of 8 Å) and the accurate particle mesh Ewald sum. The simulation cell consisted of 16 independent (10, 10) single-walled boron nitride nanotubes (SWNT) arranged in a hexagonally close packed 4×4 bundle, with periodic boundary conditions and pressure applied along all three mutually perpendicular directions. The tubes were ten unit cells long (2.3 nm). The MD simulations were carried out using the standard velocity Verlet algorithm to integrate the equations of motion. The bundles were initially equilibrated at atmospheric pressure and subsequently subjected to stepwise monotonically increasing hydrostatic pressure increments, allowing the

unit cell volume to equilibrate for at least 10 ps at each step. The simulation time step was 1 fs. Information about the structural transition was obtained by measuring the unit cell volume after equilibration at each hydrostatic pressure step. The charges on the boron and nitrogen atoms were determined by a quantum mechanical calculation done on Jaguar.¹² Three unit cells of a (10, 10) boron nitride SWNT was optimized using STO-3G basis sets for the B and the N atoms. A Mulliken population analysis was then performed for the system. The average charges on the B and N atoms belonging to the middle unit cell were found to be $0.6767e$ (B atom) and $-0.6767e$ (N atom), where e is the charge on a proton. We performed MD simulations with these values of charge as well as with zero charge on the atoms. The latter was done to ascertain the role of

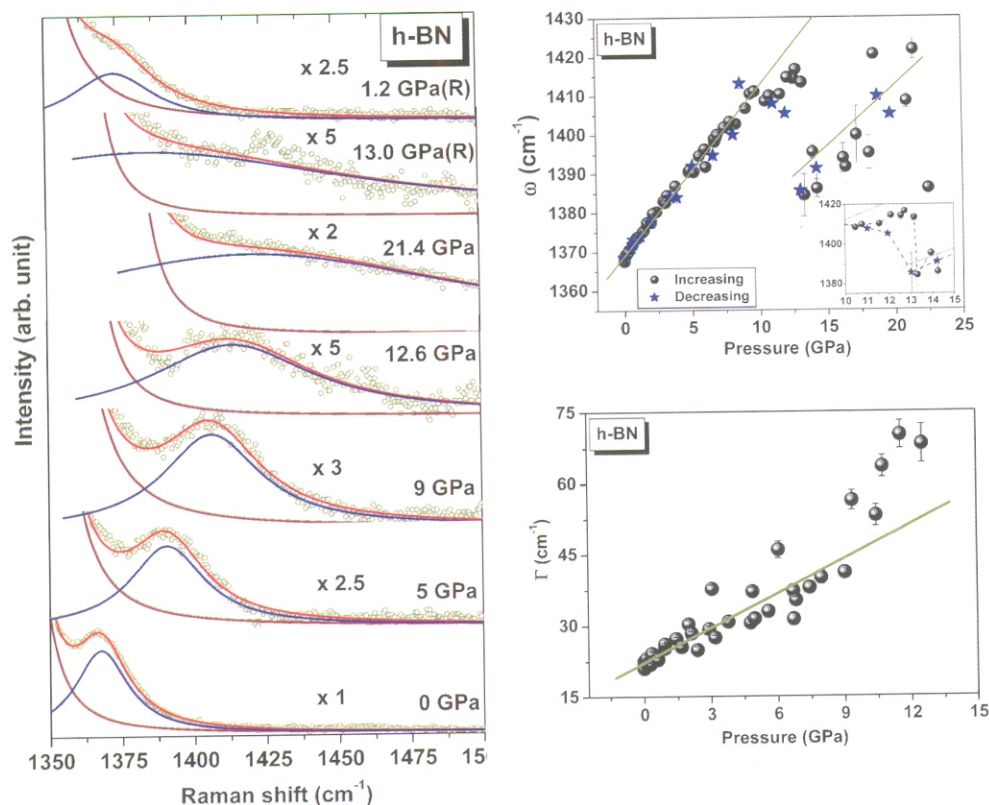


Fig. 1. Raman spectra of h-BN at various pressures, with two spectra at returned (R) pressures. The pressure dependent frequency (ω) and linewidth (Γ) are shown. The inset shows the hysteresis in frequency (ω).

charges on the atoms on the irreversible pressure-induced transformation.

4. RESULTS AND DISCUSSION

Hexagonal boron nitride has an intralayer vibrational mode at $\sim 1368 \text{ cm}^{-1}$. The effect of pressure on this mode has been followed up to 21 GPa. This Raman mode initially hardens with increasing pressure and shows a drastic drop in frequency at about 13 GPa, beyond which it again hardens with pressure (Fig. 1). This sudden change in frequency indicates a phase transition corroborated by the phase transition from hexagonal to wurtzite phase seen by X-ray diffraction^{13,14} and first principle DFT calculations.¹⁵ The transition of boron nitride is completely reversible with a small hysteresis of about 1 GPa.

Multi-walled boron nitride nanotubes with outer diameters distributed over 20–50 nm were studied up to 16 GPa by Raman spectroscopy. The spectra at different pressures are very similar to those of h-BN. With increasing pressure the intensity of the E_{2g} tangential mode decreases and vanishes completely after about 12 GPa.¹⁶ Interestingly, the mode does not recover on decompression (Fig. 2). This is in sharp contrast with the pressure behavior of multi-walled carbon nanotubes which show reversibility even after decompressing from 20 GPa² and h-BN which shows a reversible phase transition at 13 GPa. Due to strong ionic nature, the boron-nitrogen bonds are partially polarized and hence the polarized bonds on a curvature make boron nitride nanotubes $sp^{2+\alpha}$ hybridized.¹⁷ Under high pressure

when these multi-walled nanotubes collapse, the atoms with finite charge on the diametrically opposite walls of the individual tubes will have electrostatic interactions. This may be strong enough to hold the tubes in a collapsed state. We believe this may be the reason why boron nitride nanotubes get irreversibly transformed under pressure in our experiment, in contrast to carbon nanotubes. To explore the effect of charge on the pressure behavior of nanotubes, we have chosen to perform our initial molecular dynamical simulations on single-walled boron nitride nanotubes. Simulations on multi-walled nanotubes are more time intensive and will be performed at a later stage. Our preliminary results show an irreversible collapse of the tubes under some simulation conditions and reversibility under others.

For comparison purposes, we first performed molecular dynamics (MD) on a bundle of uncharged boron nitride nanotubes. To study the structural transition, we have plotted the reduced volume (V/V_0), where V_0 is the unit cell volume at atmospheric pressure, as a function of pressure as shown in Figure 3(a). The boron nitride SWNT equilibrated at atmospheric pressure has nearly circular cross sections. It is clear that the SWNT bundle undergoes a spontaneous structural transition at a critical pressure (p_c). Unless otherwise specified, p_c refers to the structural change pressure on the loading curve. Up to the critical pressure, the tube cross sections remain nearly circular with slight deformations from the circular shape. When the applied hydrostatic pressure exceeds p_c , the tube cross sections assume an elliptical shape. Further increase

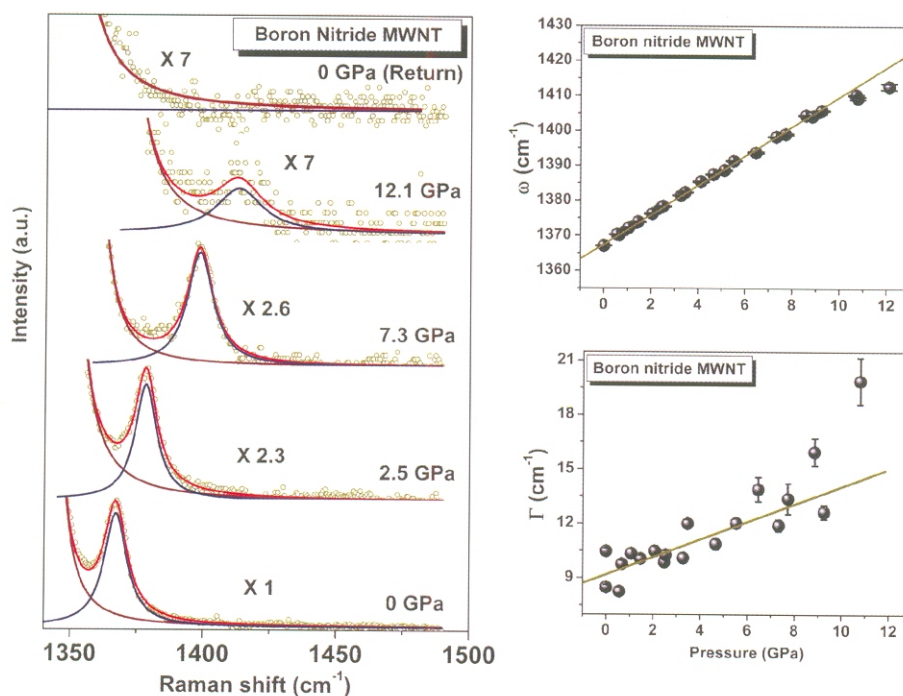


Fig. 2. Raman spectra of boron nitride multi-walled nanotubes at various pressures with the return pressure spectrum at the top panel. Pressure dependent frequency (ω) and linewidth (Γ) are also shown.

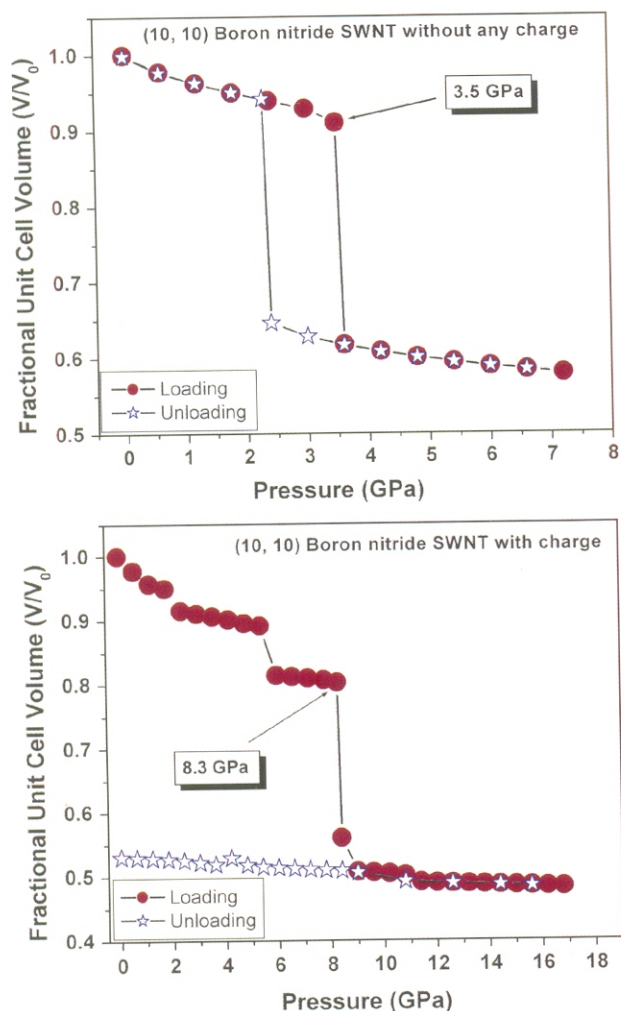


Fig. 3. Reduced volume (V/V_0) as a function of applied hydrostatic pressure for boron nitride SWNT without charge (a) and with charge (b). The loading (solid symbols) and unloading (open symbols) show hysteresis and reversibility in (a) and irreversibility in (b).

in pressure results in a dumbbell shape. Upon pressure release, the tubes undergo a reverse transformation from the collapsed to the inflated state. The loading and unloading curves show a $\sim 30\%$ hysteresis in the case of the uncharged bundle. The hexagonally close packed lattice is also completely restored on decompression. The uncharged boron nitride bundle behaves very similar to the carbon nanotube bundles.⁵

We now study the behavior of the boron nitride bundle with polar nature of the bonds under hydrostatic pressure. The electrostatic component of the interaction potential energy is computed using two different methods; the simple *cutoff* method (cutoff of 8 Å) and the accurate *particle mesh Ewald (PME)* method. Figures 4 and 5 show the nearly circular cross sections of the tubes equilibrated at atmospheric pressure studied using the cutoff and the PME methods, respectively. On plotting the reduced volume versus pressure for the bundle studied in the cutoff method, as shown in Figure 3(b), we once again observe

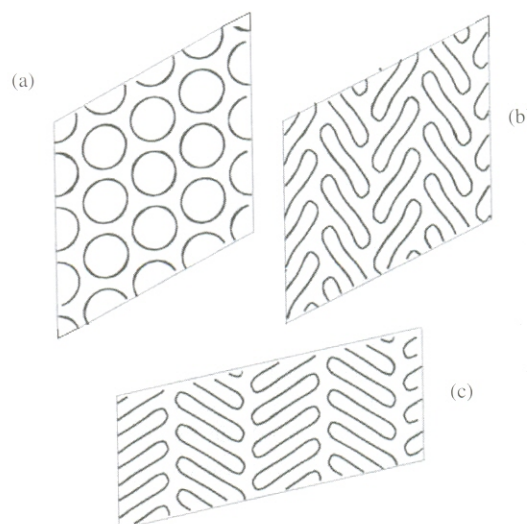


Fig. 4. Simulation of a 4×4 bundle of (10,10) boron nitride SWNT with charge (using the cutoff method). The panels show the nearly circular tube cross sections at atmospheric pressure before collapse (a), the dumbbell shaped cross sections at 9.0 GPa after collapse (b), and the collapsed structure that remains even after complete decompression (c).

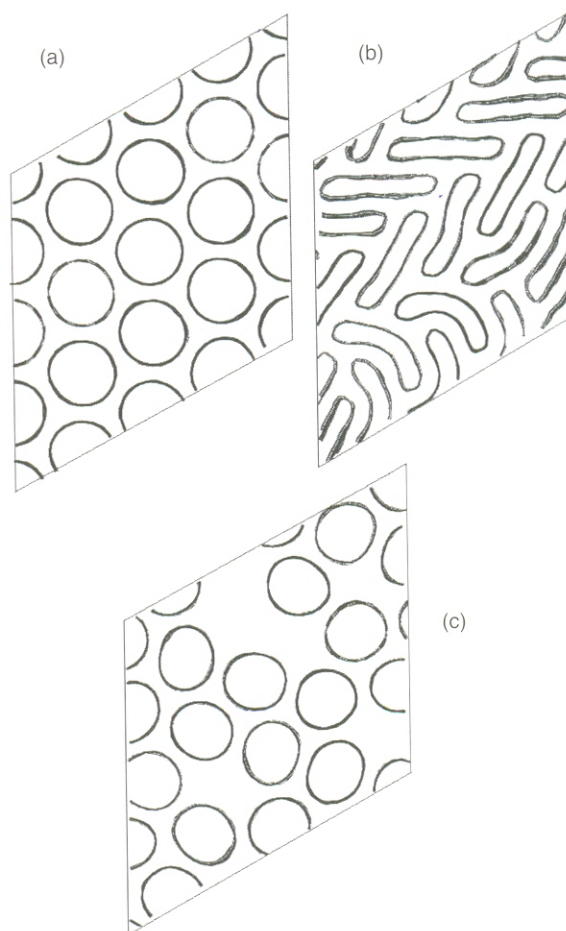


Fig. 5. Simulation of a 4×4 bundle of (10,10) boron nitride SWNT with charge (using the PME method). The panels show the nearly circular tube cross sections at atmospheric pressure before collapse (a), the dumbbell shaped cross sections at 10.0 GPa after collapse (b), and the re-inflated structure after complete decompression (c).

a clear structural transition at a well-defined critical pressure, although the p_c obtained in this case (8.3 GPa) is much higher than that obtained (3.5 GPa) in the uncharged case. Figure 4(b) shows the bundle cross section after collapse. On decompression, unlike in the uncharged case, the tubes in the bundle do not recover and continue to remain collapsed even at atmospheric pressure, as shown in Figure 4(c). The bundle studied using the more accurate PME method, however, does not show an irreversible behavior and the collapsed tubes return to their original circular cross-section on decompression, as shown in Figures 5(b) and (c). These simulations indicate that charge on the atoms does play a crucial role in determining the reversibility of boron nitride nanotubes. However, the contrasting results of the simulations performed using the cutoff and the PME methods point out that our understanding is rudimentary and more work needs to be done in this direction.

5. CONCLUSION

Our high pressure Raman spectroscopic experiments on hexagonal boron nitride and boron nitride multi-walled nanotubes suggest that h-BN undergoes a reversible phase transition to wurtzite phase at about 13 GPa and the nanotubes get irreversibly collapsed at ~ 12 GPa. Our molecular dynamics simulations on boron nitride single-walled nanotubes suggest that the polar nature of the B–N bonds may be responsible for the irreversibility of the pressure-induced transformations.

Acknowledgments: A. K. S. thanks the Department of Science and Technology, India, for financial assistance.

References and Notes

1. Pallavi V. Teredesai, A. K. Sood, D. V. S. Muthu, R. Sen, A. Govindaraj, and C. N. R. Rao, *Chem. Phys. Lett.* 319, 296 (2000).
2. S. Karmakar, S. M. Sharma, P. V. Teredesai, and A. K. Sood, *Phys. Rev. B* 69, 165414 (2001).
3. J. A. Elliott, J. K. W. Sandler, A. H. Windle, R. J. Young, and M. S. P. Shaffer, *Phys. Rev. Lett.* 92, 095501 (2004).
4. H. Zhang, D. Y. Sun, Z. F. Liu, and X. G. Gong, *Phys. Rev. B* 70, 035422 (2004).
5. Vikram Gadagkar, Prabal K. Maiti, Yves Lansac, A. Jagota, and A. K. Sood, *Phys. Rev. B* 73, 085402 (2006).
6. N. G. Chopra, R. J. Luyken, K. Cherrey, V. H. Crespi, M. L. Cohen, S. G. Louie, and A. Zettl, *Science* 269, 966 (1995).
7. A. Rubio, J. L. Corkill, and M. L. Cohen, *Phys. Rev. B* 49, 5081 (1994).
8. C. C. Tang, Y. Bando, and T. Sato, *Appl. Phys. A* 75, 681 (2002).
9. S. L. Mayo, B. D. Olafson, and W. A. Goddard III, *J. Phys. Chem.* 94, 8897 (1990).
10. MODULASIM was originally developed at the Material and Process Simulation Center, California Institute of Technology, CA, USA. <http://ruby.wag.caltech.edu/Projects/ModulaSim/index.html>. It is now actively being developed at the University of Tours (Yves Lansac), IISc, Bangalore (PKM), and University of Colorado, Boulder (Matthew A. Glaser).
11. H. J. C. Berendsen, J. P. M. Postma, W. F. van Gunsteren, A. DiNola, and J. R. Haak, *J. Chem. Phys.* 81, 3684 (1984).
12. D. J. Lockhart and P. S. Kim, *Science* 257, 947 (1992).
13. F. P. Bundy and R. H. Wentorf, Jr., *J. Chem. Phys.* 38, 1144 (1963).
14. F. R. Corrigan and F. P. Bundy, *J. Chem. Phys.* 63, 3812 (1975).
15. E. Kim and C. Chen, *Phys. Lett. A* 319, 384 (2003).
16. Surajit Saha, D. V. S. Muthu, D. Golberg, C. Tang, C. Zhi, Y. Bando, and A. K. Sood, *Chem. Phys. Lett.* 421, 86 (2006).
17. M. Machado, P. Piquini, and R. Mota, *Chem. Phys. Lett.* 392, 428 (2004).

Received: 17 April 2006. Accepted: 29 August 2006.